SCIENTIFIC REPORTS

OPEN

SUBJECT AREAS:
CHEMICAL BIOLOGY
DRUG DISCOVERY
PHARMACOLOGY
SENSORS

Received
4 May 2011

Accepted
23 June 2011

Published
7 July 2011

Correspondence and requests for materials should be addressed to Y.F. (fangy2@corning.com)

Label-free integrative pharmacology on-target of drugs at the β_2-adrenergic receptor

Ann M. Ferrie, Haiyan Sun & Ye Fang

Biochemical Technologies, Science and Technology Division, Corning Inc., Corning, NY 14831, USA.

We describe a label-free integrative pharmacology on-target (iPOT) method to assess the pharmacology of drugs at the β_2-adrenergic receptor. This method combines dynamic mass redistribution (DMR) assays using an array of probe molecule-hijacked cells with similarity analysis. The whole cell DMR assays track cell system-based, ligand-directed, and kinetics-dependent biased activities of the drugs, and translates their on-target pharmacology into numerical descriptors which are subject to similarity analysis. We demonstrate that the approach establishes an effective link between the label-free pharmacology and *in vivo* therapeutic indications of drugs.

Embraced by the "one gene, one drug, one disease" philosophy, drug development campaigns heavily invest on high throughput screening (HTS)-compatible molecular characterization assays to search maximally selective drugs ("magic bullets") for target-based therapies[1]. However, the best in class drugs are identified more by serendipity than by rational design[2], and prioritization of lead candidates is as much an art as a process[3]. This is mostly due to the poor correlation between *in vitro* results and *in vivo* indication(s). To prioritize lead candidates and predict their therapeutic potentials, biological fingerprints based on binding profiles[4], gene expression profiles[5,6], cellular phenotypic effects[7], side-effects[8], and chemical structures[9,10] can be produced so that these molecules can be directly compared and sorted. These fingerprint-based approaches are promising to relate molecular, cellular and *in vivo* features of drug molecules to targets and diseases. However, these approaches generally have poor resolution in the on-target pharmacology of a drug, the functional consequences of the drug binding to a specific target. The binding profile of a drug does not directly translate to its functional activity. The cellular phenotypic responses can differentiate antagonists from agonists, but suffer significantly in target specificity, in part due to the presence of compensatory pathways and network interactions, and in part due to the accuracy of the reference signature associated with a specific target or a cellular process[5]. Furthermore, diverse molecular assays have revealed pluridimensional efficacy (*i.e.*, an assay readout dependent efficacy) of a single drug acting through a specific target[11,12]. Since these assays measure single end points downstream the target activation, it is obviously challenging to directly compare and prioritize molecules based on multiple individual assay results, thus making it difficult to comprehend the therapeutic potential of these molecules. These problems may be overcome if it were possible to effectively cluster drugs based on their *in vitro* multifaceted on-target pharmacology.

G protein-coupled receptors (GPCRs) represent the largest and most successful class of druggable targets in human genome. This is illustrated by β-adrenergic receptors (β-ARs). The β-ARs belong to class A GPCRs and consists of β_1-, β_2- and β_3-AR subtypes. Drug development against β-ARs has been fruitful in the past several decades (Supplementary Table S1). β-blockers have been used for the treatment and management of cardiovascular conditions[13], migraine[14], and ophthalmic disorders[15], presumably due to blockage of the activation of β_1-receptor[16]. β_2-agonists have been long used in and still are the most effective bronchodilators for the treatment of asthma[17]. Several β-agonists are also used for the treatment of cardiac decompensation, anaphylaxis, sepsis, and premature labor[18]. However, neither all beta-blockers behave equally for treating various heart diseases, nor are all β_2-agonists effective in the management of asthma. Together with diverse *in vivo* indications, the distinct clinical profiles of β-drugs have challenged our view of how drugs should be classified, which, in turn, should guide us how to screen and test drugs *in vitro*[19].

Here we present a strategy to determine on-target pharmacology of drugs acting on GPCRs using label-free integrative pharmacology on-target (iPOT). Central to iPOT is label-free whole cell dynamic mass redistribution (DMR) assay[20–23]. DMR assays use a label-free optical biosensor, as shown in Fig.1a, to non-invasively record a

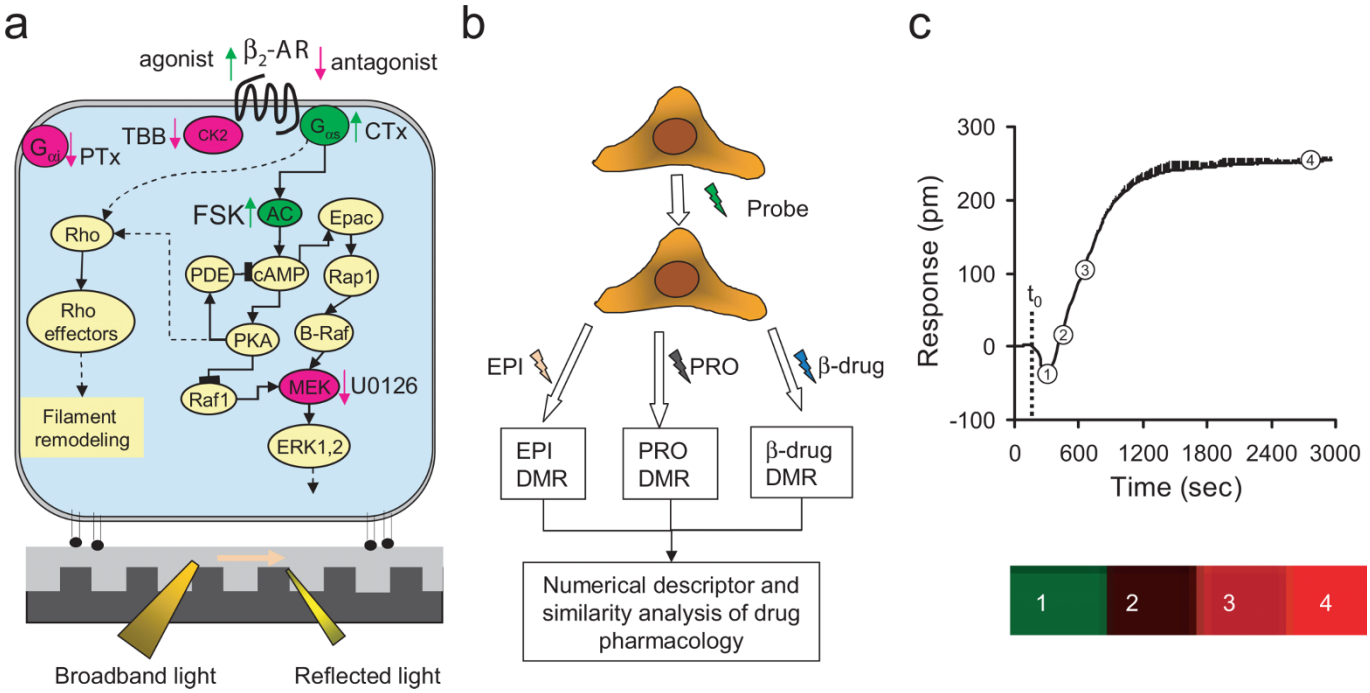

Figure 1 | The principle of the iPOT. The iPOT combines DMR assays with similarity analysis to assess on-target pharmacology of the β-AR drugs. (a) Resonant waveguide grating biosensor for receptor signaling. The biosensor uses leaky mode nano-grating waveguide structure to generate an evanescent wave to sensor whole cell responses. Cells are directly cultured onto and become adherent to the biosensor surface via adhesion complexes. A schematic of β_2-AR signaling pathway is also included. The intervention with various probe molecules of distinct signaling proteins in the β_2-AR pathway can be used as the basis to determine the on-target pharmacology of various β-drugs. (b) Assay protocols that use various probe molecules to precondition a cell expressing the β_2-AR for reporting DMR pharmacology of the β-drugs. (c) A numerical descriptor of a β-drug-induced DMR. The responses at four distinct time points were extracted and color coded. Red: positive value; green: negative value; black: close to zero. The DMR was obtained by stimulating native A431 with salmeterol at 10 μM.

drug induced dynamic redistribution of cellular matter within ~150 nm of the sensor surface[20]. The DMR is a very discerning assay that gives highly texture data at the whole cell level[19,22]. A drug-induced DMR is often sensitive to cellular context, which can be controlled using genetic manipulations or interventions with small probe molecules. DMR measurements in these perturbed cells can manifest the sensitivity of a drug-induced DMR to the target(s)/pathway(s) with which the small probe molecules intervene. Combining DMR assays in a wide array of probe molecule perturbed cells with similarity analysis can separate drugs based on their distinct on-target pharmacology. We demonstrate that this strategy provides an effective link between *in vitro* profiles and *in vivo* indications of β-drugs.

Results

The principle of iPOT. The iPOT begins with the use of diverse probe molecules to hijack a cell or cell system, followed by profiling drugs with DMR assays. The DMR profiles obtained for each drug are then translated to a multi-dimensional coordinate such that all drugs tested can be compared using similarity analysis. The probes are chosen to recapitulate signaling pathways downstream the target as well as pharmacological activities of drugs, such that the pathway biased activity, if any, of drugs can be systematically surveyed. The probes can be toxins for G proteins, inhibitors for kinases and activators for enzymes within the receptor signaling cascades, or β-drugs themselves (Fig.1a). The DMR arising from β-drugs in the probe pretreated cells are used directly for similarity analysis, except that when the probes are β-drugs, the DMR arising from epinephrine or propranolol are used as readouts (Fig.1b; Table 1). The cell or system is chosen based on the known signaling capacity of the target, although the cells that are derived from *in vivo* action sites of the drugs can be used. Hijacking of the cell with the probes redirects the signaling routes of the target, thus manifesting the biased activity of drugs towards the probe-intervened pathways. After translating the kinetic DMR profiles into multidimensional coordinates, similarity is analyzed to categorize drugs into distinct clusters. We assume that drugs within a given (sub)cluster share a common mode of action possibly linked to an *in vivo* indication. The iPOT effectively integrates the system-based, ligand-directed, and kinetics-dependent biased activities of the drugs.

iPOT profiles established a link between *in vitro* results and *in vivo* indications of β-drugs. We implemented the iPOT to characterize all β-drugs approved by the Food and Drug Administration (FDA) (Supplementary Table S2). All β_2-drugs were profiled at 10 μM to achieve maximal signaling capacity and to be amenable for HTS (Supplementary Table S3). Human epidermoid carcinoma A431 was chosen to be the cell system since its endogenous β_2AR has been served as a model to elucidate the β_2AR signaling in the past[24]. Before measuring the DMR induced by β-drugs, A431 was preconditioned under eight different conditions: (1) the assay vehicle for 1 hr as a control; (2) 1 μM propranolol (PRO) for 1 hr; (3) 5 nM epinephrine (EPI) for 1 hr; (4) 5 nM EPI for 5 hrs; (5) 400 ng/ml Chorea toxin (CTx) for overnight; (6) 100 ng/ml Pertussis toxin (PTx) for overnight; (7) 10 μM 4,5,6,7-tetrabromo-benzotriazole (TBB) for 1 hr; and (8) 10 μM U0126 for 1 hr. We also measured the EPI DMR in cells after pretreated with 10 μM β-drugs for 1 hr or 5 hrs, the β-drug DMR in the presence of 10 μM forskolin (FSK), and finally the PRO DMR in cells after pretreated with 10 μM β-drugs for 5 hrs (Fig.1b). Total twelve DMR profiles were collected for each drug (Table 1).

Table 1 | Assay protocols and DMR signals used for similarity and correlation analysis.

Assay number	Probe, pretreatment duration	DMR readout	Note
1	0.1% DMSO, 1hr	Ligand, 10 μM	Positive control, agonism
2	10 μM Ligand, 1hr	Epinephrine, 5 nM	Specificity, relative potency and efficacy, modes of action
3	1 μM propranolol, 1hr	Ligand, 10 μM	Specificity, relative potency and efficacy, modes of action
4	5 nM Epinephrine, 1hr	Ligand, 10 μM	Receptor desensitization and deactivation
5	10 μM ligand, 5hr	Epinephrine, 5nM	Kinetics dependent receptor blockage by antagonists and receptor desensitization by agonists
6	5 nM Epinephrine, 5hr	Ligand, 10 μM	Kinetics dependent deactivation of the receptor after prolonged activation with epinephrine
7	10 μM ligand, 5hr	Propranolol, 10 μM	Relative potency, kinetics dependent agonism
8	0.1% DMSO, 1hr	Forskolin 10 μM Ligand, 10 μM	cAMP-PKA pathway
9	400 ng/ ml cholera toxin, 20hr	Ligand, 10 μM	$G_{\alpha s}$-dependent and independent activity
10	100 ng/ml pertussis toxin, 20hr	Ligand, 10 μM	$G_{\alpha i}$ sensitivity
11	10 μM TBB, 1hr	Ligand, 10 μM	CK2 sensitivity
12	10 μM U0126, 1hr	Ligand, 10 μM	MEK1/2 sensitivity

Each DMR profile is a kinetics response with more than 200 time points. To improve the efficiency of similarity analysis, we reduced the DMR dimensions to four distinct time points (3, 5, 9, and 45 min post stimulation) (Fig.1c). The dimension reduction is based on clustering of time domains of the DMR of all β-drugs in the DMSO treated cells (Supplementary Fig.S1). Results showed that the β-drug DMR generally propagate with four distinct time periods: immediate (2–4 min), early (5–6 min, and 7–9 min), and late responses (10–60min post stimulation). Similar pattern was obtained for all DMR signals under all twelve conditions. Thus, we selected one time point from each period to represent each DMR, and we found that these time points adequately represent the key features of the drug responses (Supplementary Fig.S2 and S3). Thus, the twelve DMR profiles of each drug can be rewritten into a 48 dimensional coordinate.

Similarity analysis using unsupervised Ward hierarchical clustering algorithm and Euclidean distance metrics[25] categorized drugs into distinct clusters (Fig.2). Detailed analysis revealed several interesting aspects. First, the DMR assays are high quality in general, since two isomers and their mixture of propranolol led to subtle difference in DMR profiles but were still bucketed together; and the same was true for S-isomer and its mixture of pindolol. Further, the β_2-inactive R-(+)-atenolol was clearly different from its active isomer, S(-)-atenolol. R-(+)-atenolol was clustered with practolol and the negative control dimethyl sulfoxide (DMSO). Practolol is a β_1-selective but much less potent β_2-antagonist. Second, two superclusters were formed; one for partial agonists and antagonists, and another for strong partial agonists, full agonists and the adenylyl cyclase activator forskolin (FSK). Each supercluster is further divided into many subclusters. Third, drugs in each subcluster share almost identical therapeutic indications as approved by the FDA and documented in DrugBank[26], and the correlation between DMR profiles and *in vivo* indications was correctly established for more than 90% of the drugs tested. Notable disassociations between the DMR profiles and original indications were: (1) carvedilol was clustered with PRO. A small but positive clinical trial using carvedilol for the prophylactic treatment of migraine has been reported in literature[27]. (2) Terbutaline was close to ritodrine, and to less degree, phenylephrine. Although it is controversial and has not been approved by the FDA for tocolytic use, terbutaline is the most widely prescribed beta-mimetic to arrest or prevent premature labor in the United States[18]. (3) Salmeterol was distinct from all other anti-asthma agonists. (4) Timolol was distinct from PRO although timolol is also used for treating migraine. (5) The active metabolite (methylnorepinephrine) of methyldopa was close to norepinephrine.

We further compared the results obtained with DMR profiles with those obtained using *in vivo* indications or chemical features. Clustering of β-drugs based on their *in vivo* indications, as documented in DrugBank, led to a relatively low resolution heat map (Fig.3a). For this analysis, a binary numeral system, 1 for an approved indication and 0 for none, is used to describe each drug based on their clinical indications. We also analyzed the chemical similarity of all β-drugs tested using ChemMine[28]. ChemMine is an online service for analyzing and clustering small molecules. Chemical similarity based on Tanimoto coefficient led to bucketing of compounds that shows relatively poor correlation with their *in vivo* indications (Fig.3b). These comparative analyses suggest that the iPOT gave rise to better correlation between *in vitro* results and *in vivo* indications.

Correlation analysis identified the origin of similarity among β-drugs. We used correlation analysis between distinct conditions to further determine the origin of similarity/difference among β-drugs. We used seven assays to separate β-drugs based on agonism, specificity, potency, and kinetics-dependent mechanisms of activation and inactivation. First, we recorded the DMR arising from all drugs in the native cells. Results showed that there were three classes of drugs: full agonists that triggered a DMR similar to the EPI DMR; partial agonists that led to a DMR smaller than the EPI DMR; and apparent inactive drugs that led to a net-zero DMR (Supplementary Fig.S3). Second, we examined the impacts of β-drugs on the succeeding EPI DMR, wherein the cells were pretreated with β-drugs for 1hr or 5hr. Results suggest that S-(-)-atenolol, (±)atenolol and practolol exhibited weak antagonism, while dobutamine and dopamine led to weak agonism, but R-(+)-atenolol was inactive (Fig.4a). However, the EPI DMR after the cells were pretreated with β-drugs for 5hr showed that dobutamine and dopamine caused a complete desensitization, but bisprolol and acebutolol led to a reduced blockage of the succeeding EPI DMR (Fig.4a; supplementary Fig.S4). Third, we examined the DMR induced by β-drugs after the cells were pre-activated with 5 nM EPI for 1 hr or 5hr. Results showed that there was a linear correlation between the two DMR for most β-drugs (Fig.4b). The drugs in the cells after the longer EPI pretreatment generally led to a more positive DMR. However, the DMR arising from satolol, R(+)atenolol, carvedilol, and (±)-, R-(+)- and S-(-)-propranolol were largely insensitive to the pretreatment duration with EPI (Fig.4b; Supplementary Fig.S5 and S6). Fourth, we examined the ability of PRO to block the DMR arising from β-drugs, wherein PRO was used to pre-stabilize the receptor at its inactive conformation. This further separated β-drugs based on potency (Fig.5a). The percentage of inhibition by PRO was mostly inversely correlated with the potency (*i.e.*, K_i or $EC_{50,\ cAMP}$) of an agonist drug, except for a group of partial agonist drugs that include pindolol, alprenolol, oxprenolol, labetalol and isoetharine (Supplementary

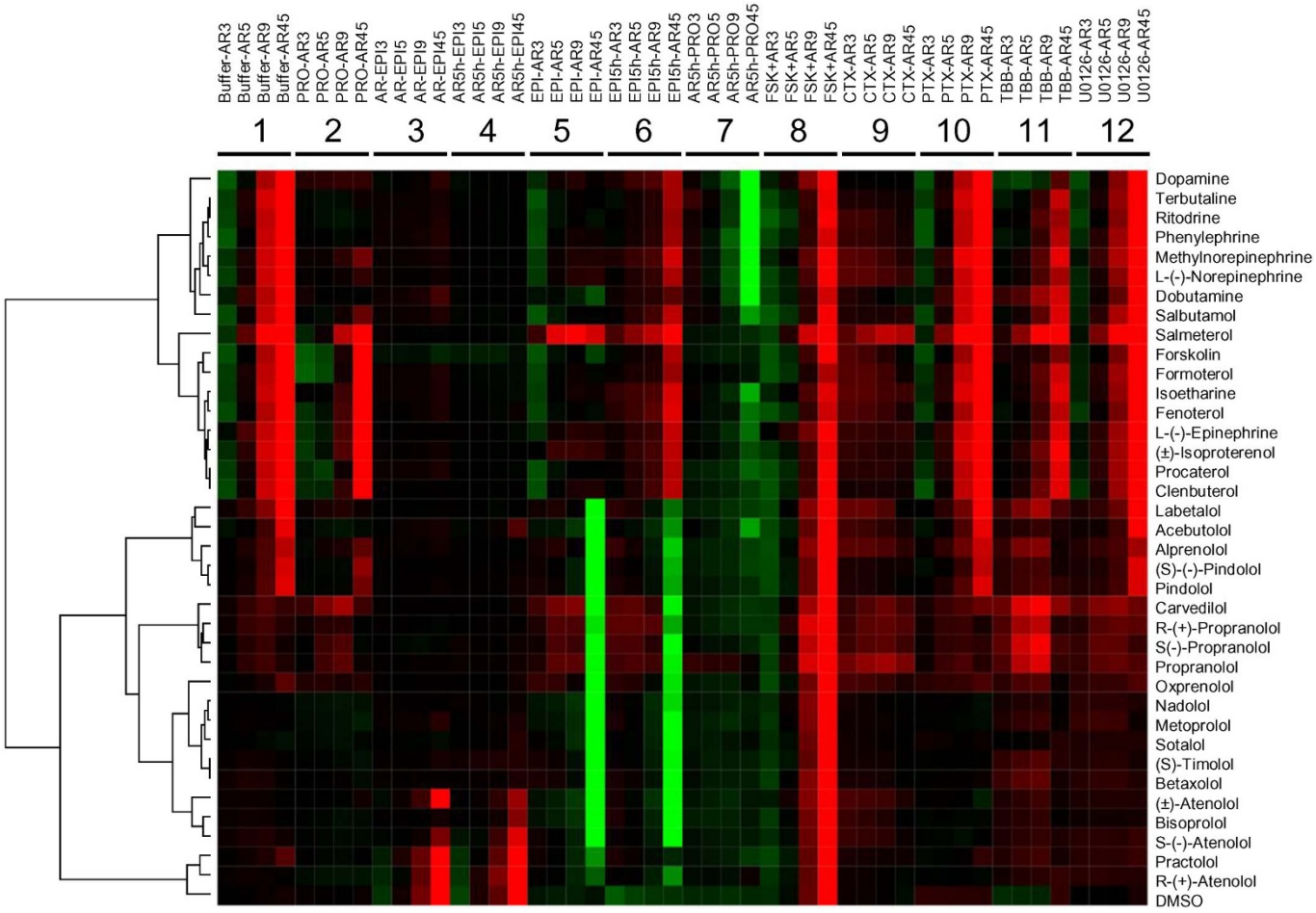

Figure 2 | DMR heat map of clinically available β-drugs. This heat map was obtained using DMR profiling of the drugs under twelve conditions, followed by similarity analysis using the Ward hierarchical clustering algorithm and Euclidean distance metrics. The twelve DMR used for analysis were: a drug-induced DMR in the cells pretreated with the assay vehicle for 1 hr (Buffer – AR), 1 μM propranolol for 1 hr (PRO – AR), 5 nM EPI for 1 hr (EPI – AR), 5 nM EPI for 5 hrs (EPI5h – AR), 400 ng/ml CTx for overnight (CTx – AR), 100 ng/ml PTx for overnight (PTx – AR), 10 μM TBB for 1 hr (TBB – AR), and 10 μM U0126 for 1 hr (U-126 – AR). In addition, we also included an EPI-induced DMR in the cells pretreated with 10 μM β-drugs for 1 hr (AR – EPI) and for 5 hrs (AR5h – EPI); an PRO-induced DMR in the cells pretreated with 10 μM β-drugs for 5 hrs (AR5h – PRO); and a forskolin (FSK)-induced DMR in the presence of β-drugs (FSK + AR).

Fig.S7). Finally, we examined the ability of PRO to alter the course of a drug-induced DMR after the drug was exposed to the cells for 5 hrs (Fig.5b). This further separated agonist drugs, in which PRO reversed the DMR arising from distinct agonist drugs to different degrees (Supplementary Fig.S8).

Next, we used three assays to delineate drug pharmacology based on G protein-dependent and independent signaling. First, we examined the DMR induced by FSK in the absence and presence of a β-drug (Fig.6a), wherein FSK was used to activate adenylyl cyclases. This delineated drugs into three groups: drugs that suppressed the FSK DMR, drugs that potentiated the FSK DMR with an accelerated kinetics, and drugs that had little impact on the FSK DMR (Supplementary Fig.S9). Notable is salmeterol which significantly potentiated the FSK DMR, unlike all other strong partial and full agonists. Second, we compared the β-drug DMR without and with the pre-decoupling of $G_{\alpha s}$ proteins from the receptor by CTx (Fig.6b). This identified drugs that still produced noticeable DMR (e.g., EPI, alprenolol), or led to an increased DMR (e.g., carvedilol) in the CTx-pretreated cells (Supplementary Fig.S10). Third, we compared the β-drug DMR without and with the masking of $G_{\alpha i}$ proteins by PTx (Fig.7a). This resulted in a linear correlation between the two DMR, but with a slope of 0.95, suggesting that the impairment of $G_{\alpha i}$ by PTx suppressed all β-drug-induced DMR.

Finally, we used three assays to probe ligand-directed biased agonism. First, we used a MEK1/2 inhibitor U0126 to inhibit the activity of MEK1/2. This led to a linear correlation with a slope significantly greater than 1 between the two DMR arising from β-drugs without and with the U0126 pretreatment (Fig.7a). This also identified practolol and oxprenolol, both of which led to a suppressed DMR by U0126 (Supplementary Fig.S11). Second, we examined the impacts of a Casein kinase (CK2) inhibitor TBB on the drug-induced DMR (Fig.7b), wherein TBB was used to precondition the cells with suppressed CK2 activity. Distinct drugs exhibited different sensitivities to the TBB treatment (Supplementary Fig.S12). Third, we compared a drug-induced DMR with its whole cell cAMP signal (Fig.8). This identified DMR-biased drugs including practolol, alprenolol, pindolol, labetalol, acebutolol, and dopamine. Dopamine was previously shown to be moderately potent to trigger DMR signal in A431 cells[29].

Discussion

In contrast to conventional molecular assays that are biased towards a single pathway and/or a single molecule, the integrative readout of DMR assays allows assessing drug pharmacology with wide pathway coverage. The imminent high temporal resolution makes DMR assays possible to quantify drug pharmacology at different time domains. The non-invasive measure enables DMR assays to probe

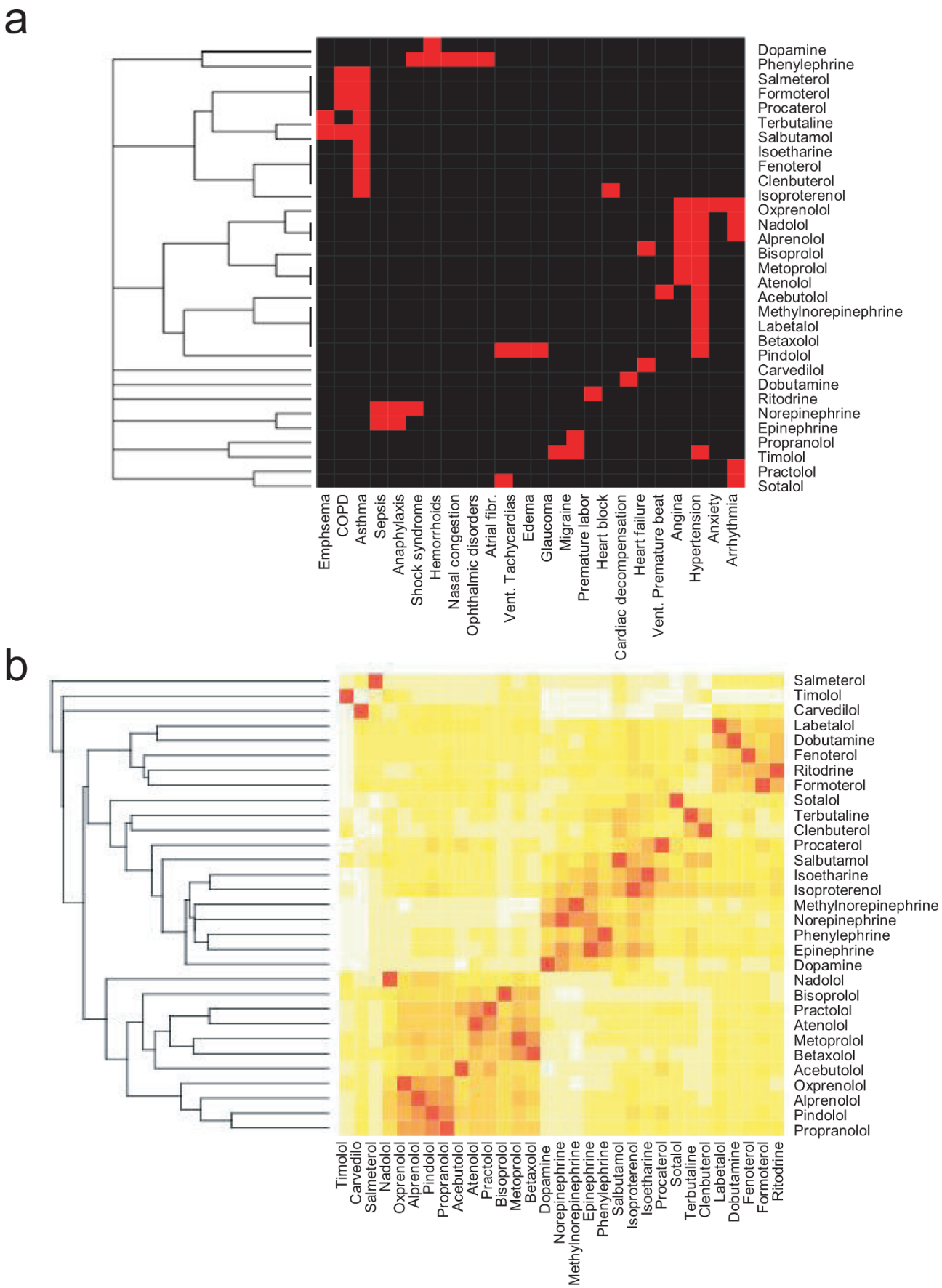

Figure 3 | **Heat maps of β-drugs.** (a) Clinical indications of all drugs were used as a basis for similarity analysis. (b) Chemical structures of all drugs were used as a basis for similarity analysis.

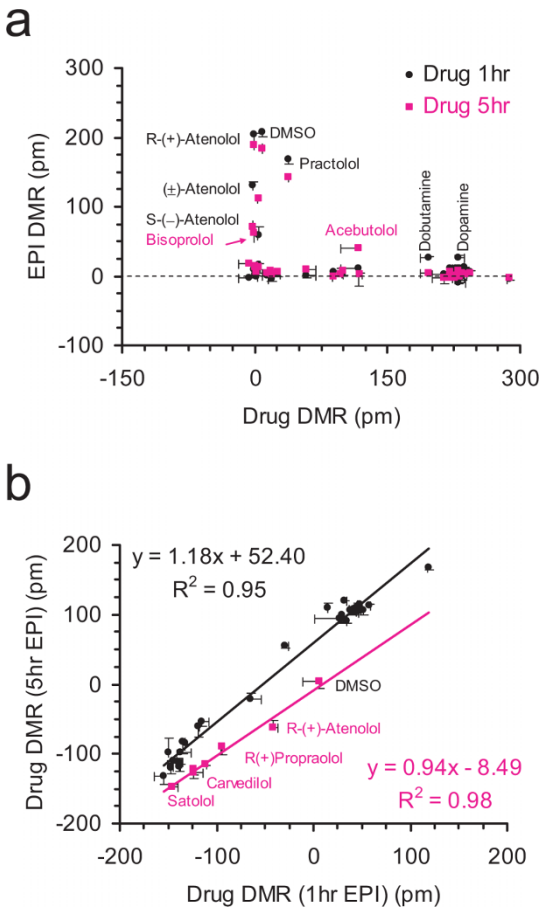

Figure 4 | Correlation analysis identifies the origin of similarity among distinct β-drugs based on potency, mechanisms of activation and deactivation. (a) Scatter plots between the β-drug-induced DMR in native cells and the EPI-induced DMR after pretreated with drugs for 1hr (black dots) or 5hr (pink dots); and (b) scatter plots between the β-drug-induced DMR in cells after pretreatment with EPI for 1hr and 5hr.

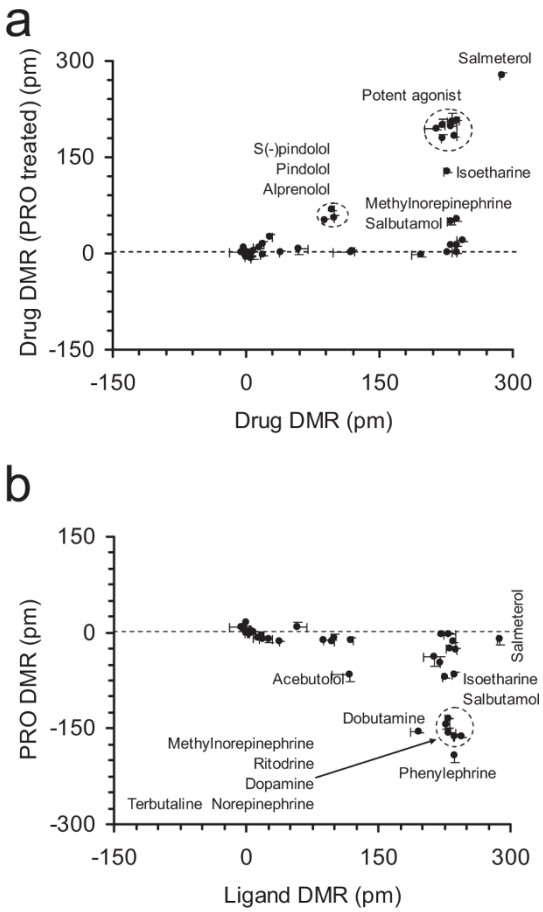

Figure 5 | Correlation analysis identifies the origin of similarity among distinct β-drugs based on potency, mechanisms of activation and deactivation. (a) Scatter plots between the β-drug-induced DMR without and with the pretreatment with PRO for 1hr; (b) scatter plots between the β-drug-induced DMR in native cells and the PRO-induced DMR in the cells after 5hr pretreatment with β-drugs.

drug pharmacology under a wide range of conditions. The DMR assays are robust and reproducible (Supplementary Fig.S13). Combining DMR assays with similarity analysis can differentiate drug pharmacology with relatively high resolutions. We implanted the iPOT to investigate the pharmacology of clinically available β-AR drugs. Using twelve DMR assays in a cell line endogenously expressing the β_2-AR under distinct chemical environments, we found that clinically approved β-AR drugs are divergent in their potency, mechanisms of activation and inactivation, and pathway biased activity. Although only a first step, our results are encouraging. The most notable finding is that the iPOT profiling of β-AR drugs established an apparently effective link between *in vitro* results and *in vivo* indications. iPOT profiles of drugs in disease relevant cells, together with global analysis of drugs against the family of adrenergic receptors, would further strengthen the correlation between *in vitro* and *in vivo* results.

Since DMR is an integrated measure of receptor signaling, specific biological events that underlie the similarity and differences among distinct drugs are still largely unknown[30]. The linkage between a specific DMR parameter and a specific clinical feature is also largely unknown at the present time. Further delineation of receptor biology and drug pharmacology, together with optimization of algorithm for similarity analysis, would be necessary to validate the link between the iPOT testing results and *in vivo* indications, and to make it possible to rank and select drugs within a class for *in vivo* testing during lead selection process. Nonetheless, the high content assessment of drug pharmacology with label-free iPOT assays elucidates the complex and multifaceted efficacy of GPCR ligands, thus offering a practical process to reposition drugs for new indications [31,32] and to prioritize lead molecules.

Methods

Cell lines and reagents. Human epidermoid carcinoma A431 was obtained from American Type Cell Culture. The cells were grown in Dulbecco's modified Eagle's medium (DMEM) supplemented with 10% fetal bovine serum (FBS), 4.5g/liter glucose, 2 mM glutamine, and antibiotics. The native cells were passed when approaching ~90% confluence with trypin/EDTA (etthylenediaminetetraacetic acid) to provide new maintenance cultures on T-75 flasks and experimental cultures on the biosensor microplates. All drug molecules were purchased from commercial sources (Supplementary Table S2). All drugs were dissolved in DMSO and were diluted directly into the assay buffer (1× Hanks' balanced salt buffer, 20mM Hepes, pH 7.1; HBSS) to the indicated concentrations. Epic® 384-well tissue culture treated biosensor microplates were obtained from Corning Incorporated (Corning, NY, USA).

DMR assays. Epic® system (Corning Inc.), a wavelength interrogation reader system tailored for resonant waveguide grating (RWG) biosensors in microtiter plates, was used for all DMR assays. This system consists of a temperature-control unit (26°C), an optical detection unit, and an on-board liquid handling unit with robotics. The detection unit is centered on integrated fiber optics, and enables kinetic measures of cellular responses with a time interval of ~15sec. 20,000 cells per well were directly seeded and cultured overnight under serum rich medium, followed by starvation overnight using serum depleted medium. After washed twice, the cells were maintained with HBSS and further incubated inside the system for 1hr. A 2-min baseline was then established. Immediate after the compound additions using the onboard liquid handler, the cellular responses were recorded. All studies were carried out with at least three replicates.

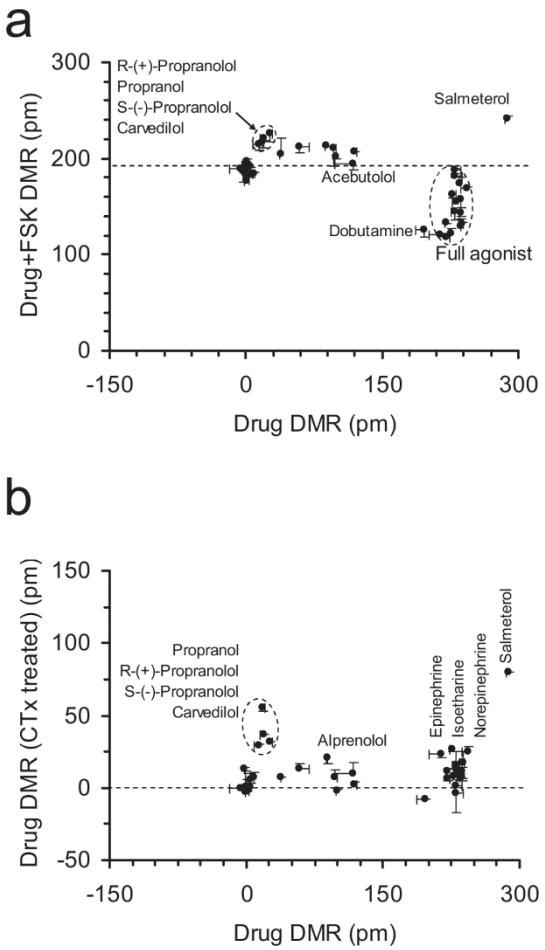

Figure 6 | Correlation analysis identifies the origin of similarity among distinct β-drugs based on pathway biased agonism. (a) Scatter plot between the β-drug-induced DMR in native cells and the FSK DMR in the presence of distinct β-drugs; (b) Scatter plot between the β-drug-induced DMR in native cells and in the cells after pretreatment with CTx.

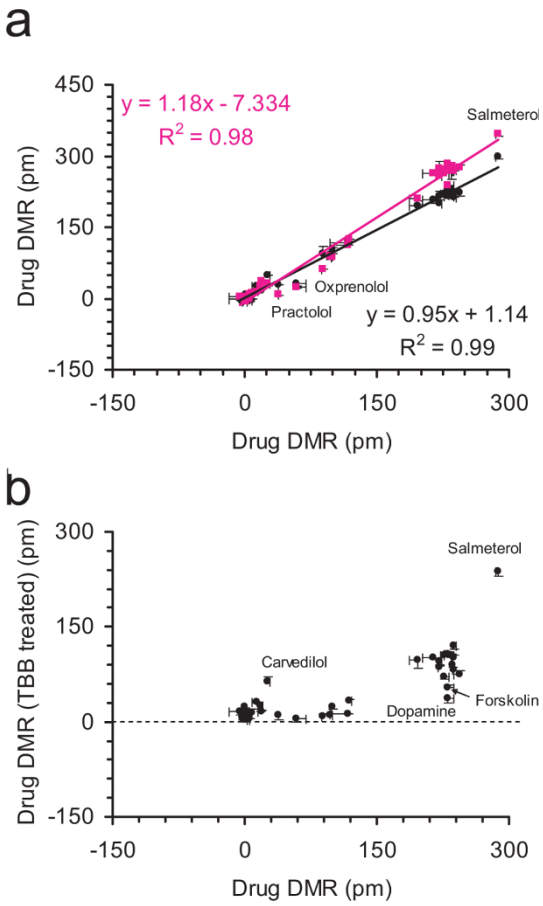

Figure 7 | Correlation analysis identifies the origin of similarity among distinct β-drugs based on pathway biased agonism. Scatter plots between the β-drug-induced DMR in native cells and in the cells after pretreatment with PTx (black dots) or U0126 (pink dots) (a), and TBB (b).

Drug screening. We screened all 36 clinically available β-AR drugs and drug isomers against 12 distinct assay conditions using kinetic DMR assays. Drug concentrations were chosen to achieve maximum efficacy and to be amenable for high throughput screening (Supplementary Table S3). A431 cells were preconditioned with probe molecules to achieve a wide range of chemical environments, which, in turn, manifest the specificity, relative potency and efficacy, and modes of action of the drugs. The chemical environments also enable mapping the cell systems-based, ligand-directed and kinetics-dependent biased agonism of the drugs. Specifically, cells were pretreated with DMSO (the positive control), 5nM epinephrine, 1μM propranolol, 400ng/ml cholera toxin, 100ng/ml pertussis toxin, U0126, 4,5,6,7-tetrabromobenzotriazole, forskolin, and the drug molecules for a specific period of time (Table 1). Afterwards, cells were stimulated with a β_2-ligand (epinephrine, propranolol, or the drug), whose responses were recorded in real time and used for similarity and correlation analysis.

Whole cAMP assays. Cells were plated in 384well tissue culture treated plates (BD Bioscience, Cat# 354660) with a seeding density of 20000 cells per well. Cells were cultured in the serum rich medium overnight. The next day cAMP-Glo assay was performed according to manufacturer's instruction (Promega, Cat#V1502). Cells were incubated with 10 μM compounds in induction buffer for 30 minutes before adding lysis buffer. Luminescence was measured using Tecan SafireII reader.

Data visualization and clustering. For each DMR the responses at the four distinct time points (Fig.1c) were extracted for reduction of the time dimensions. All time points refer to the stimulation duration after renormalized the responses starting from t_0 (the time when the compound was added) (Fig.1c). For visualization purpose the responses were color coded to illustrate relative differences in DMR signal strength. The total 48 dimensions, 4 for each condition, were thus obtained to rewrite the DMR pharmacology of a drug. In the drug matrix (Fig. 2) each column represents one DMR response at a particular time in a specific assay condition, and each row represents one drug with the original approved indications, as documented in DrugBank (Http://www.drugbank.ca). Every row and column carries equal weight. The Ward hierarchical clustering algorithm and euclidean distance metrics (http://www.eisenlab.org/eisen/) were used for clustering the results. DMSO in the vehicle, a concentration that equals to those for all drugs, is also included as a negative control. For replicates, we used statistical differences using the four chosen time points to calculate the variability among replicates. All replicates have to pass the 2× coefficient of variation test before being included in analysis. The drugs whose DMR responses failed the test are re-screened. For clinical indications, each drug was written using a binary numeral system, 1 for a clinical indication as documented in DrugBank and 0 for none. For chemical structures, all drugs were analyzed using ChemMine online software, which employs atom pairs as structural descriptors and Tanimoto coefficient as a similarity measure. Hierarchical clustering was used for clustering based on both clinical features and chemical structures.

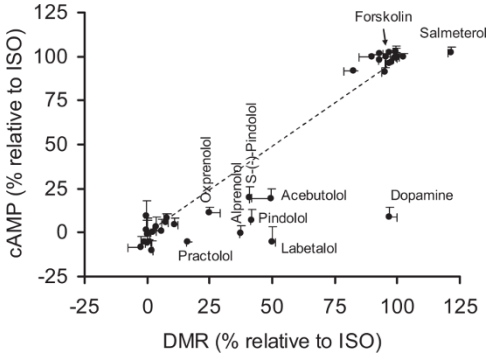

Figure 8 | Correlation between the β-drug-induced DMR in native cells and the whole cell cAMP level induced by β-drugs.

1. Strebhardt, K. & Ullrich, A. Paul Ehrlich's magic bullet concept: 100 years of progress. *Nat. Rev. Cancer* **8**, 473–480 (2008).
2. Butcher, E. Can cell systems biology rescue drug discovery? *Nat. Rev. Drug Discov.* **4**, 461–467 (2005).
3. Gleeson, M., Hersey, A., Montanari, D. & Overington, J. Probing the links between in vitro potency, ADMET and physicochemical parameters. *Nat. Rev. Drug Discov.* **10**, 197–208 (2011).
4. Fliri, A. F., Loging, W. T., Thadeio, P. F. & Volkmann, R. A. *Proc. Natl. Acad. Sci. USA* **102**, 261–266 (2005).
5. Lamb, J., Crawford, E. D., Peck, D., Modell, J. W., Blat, I. C., Wrobel, M. J., Lerner, J., Brunet, J. P., Subramanian, A., Ross, K. N., Reich, M., Hieronymus, H., Wei, G., Armstrong, S. A., Haggarty, S. J., Clemons, P. A., Wei, R., Carr, S. A., Lander, E. S. & Golub, T. R. The Connectivity Map: using gene-expression signatures to connect small molecules, genes, and disease. *Science* **313**, 929–35 (2006).
6. Hoon, S., Smith, A. M., Wallace, I. M., Suresh, S., Miranda, M., Fung, E., Proctor, M., Shokat, K. M., Zhang, C., Davis, R. W., Giaever, G., St Onge, R. P. & Nislow, C. An integrated platform of genomic assays reveals small-molecule bioactivities. *Nat. Chem. Biol.* **4**, 498–506 (2008).
7. Young, D. W., Bender, A., Hoyt, J., McWhinnie, E., Chirn, G.-W., Tao, C. Y., Tallarico, J. A., Labow, M., Jenkins, J. L., Mitchison, T. J. & Feng, Y. Integrating high-content screening and ligand-target prediction to identify mechanism of action. *Nat. Chem. Biol.* **4**, 59–68 (2008).
8. Campillos, M., Kuhn, M., Gavin, A., Jensen, L. & Bork, P. Drug target identification using side-effect similarity. *Science* **321**, 263–266 (2008).
9. Keiser, M. J. Setola, V., Irwin, J. J., Laggner, C., Abbas, A. I., Hufeisen, S. J., Jensen, N. H., Kuijer, M. B., Matos, R. C., Tran, T. B., Whaley, R., Glennon, R. A., Hert, J., Thomas, K. L. H., Edwards, D. D., Shoichet, B. K. & Roth, B. L. Predicting new molecular targets for known drugs. *Nature* **462**, 175–181 (2009).
10. Zhao, S. & Li, S. Network-based relating pharmacological and genomic spaces for drug target identification. *PLoS One* **5**, e11764 (2010).
11. Galandrin, S. & Bouvier, M. Distinct signaling profiles of β_1 and β_2 adrenergic receptor ligands toward adenylyl cyclase and mitogen-activated protein kinase reveals the pluridimensionality of efficacy. *Mol. Pharmacol.* **70**, 1575–1584 (2006).
12. Kenakin, T. & Miller, L. J. Seven transmembrane receptors as shapeshifting proteins: the impact of allosteric modulation and functional selectivity on new drug discovery. *Pharmacol. Rev.* **62**, 265–304 (2010).
13. Expert consensus document on β-adrenergic receptor blockers: The task force on beta-blockers of the European Society of Cardiology. *Euro. Heart J.* **25**, 1341–1362 (2004).
14. Mehrotra, S., Gupta, S., Chan, K. Y., Villalon, C. M., Centurion, D., Saxena, P. R., Maassen, A. Current and prospective pharmacological targets in relation to antimigraine action. *Naunyn-Schmiedeberg's Arch Pharmacol.* **378**, 371–394 (2008).
15. Hayreh, S. S., Podhajsky, P. & Zimmerman, M. B. Beta-blocker eyedrops and nocturnal arterial hypotension. *Am. J. Ophthalmol.* **128**, 301–309 (1999).
16. Cruickshank, J. M. Beta-blockers continue to surprise us. *Euro. Heart J.* **21**, 354–364 (2000).
17. Nguyen, L. P., Lin, R., Parra, S., Omoluabi, O., Hanania, N. A., Tuvim, M. J., Knoll, B. J., Dickey, B. F. & Bond, R. A. β_2-Adrenoceptor signaling is required for the development of an asthma phenotype in a murine model. *Proc. Natl. Acad. Sci. USA* **106**, 2435–2440 (2009).
18. Lam, F. & Gill, P. Beta-agonist tocolytic therapy. *Obstet. Gynecol. Clin. North Am.* **32**, 457–484 (2005).
19. Kenakin, T. Cellular assays as portals to seven-transmembrane receptor-based drug discovery. *Nat. Rev. Drug Discov.* **8**, 617–626 (2009).
20. Fang, Y., Ferrie, A. M., Fontaine, N. H., Mauro, J. & Balakrishnan, J. Resonant waveguide grating biosensor for living cell sensing. *Biophys. J.* **91**, 1925–1940 (2006).
21. Fang, Y., Ferrie, A. M., Fontaine, N. H. & Yuen, P. K. Characteristics of dynamic mass redistribution of epidermal growth factor receptor signaling in living cells measured with label-free optical biosensors. *Anal. Chem.* **77**, 5720–5725 (2005).
22. Fang, Y. Label-free receptor assays. *Drug Discov. Today Technol.* **7**, e5–e11 (2010).
23. Schröder, R., Janssen, N., Schmidt, K., Kebig, A., Merten, N., Hennen, S., Müller, A., Blättermann, S., Mohr-Andrä, M., Zahn, S., Wenzel, J., Smith, N. J., Gomeza, J., Drewke, C., Milligan, G., Mohr, K., Kostenis, E. Deconvolution of complex G protein-coupled receptor signaling in live cells using dynamic mass redistribution measurements. *Nat. Biotechnol.* **28**, 943–949 (2010).
24. Tran, T. M., Friedman, J., Qunaibi, E., Baameur, F., Moore, R. H. & Clark, R. B. Characterization of agonist stimulation of cAMP-dependent protein kinase and G protein-coupled receptor kinase phosphorylation of the β_2-adrenergic receptor using phosphoserine-specific antibodies. *Mol. Pharmacol.* **65**,196–206 (2004).
25. Eisen, M. B., Spellman, P. T., Brown, P. O. & Botstein, D. Cluster analysis and display of genome-wide expression patterns. *Proc. Natl. Acad. Sci. USA* **95**, 14863–14868 (1998).
26. Wishart, D. S., Knox, C., Guo, A. C., Cheng, D., Shrivastava, S., Tzur, D., Gautam, B. & Hassanali, M. DrugBank: a knowledgebase for drugs, drug actions and drug targets. *Nucl. Acids Res.* **36**, D901–D906 (2007).
27. Bigal, M. E. & Krymchantowski, A. V. Emerging drugs for migraine prophylaxis and treatment. *Med. Gen. Med.* **8**, 31 (2006).
28. Cao, Y., Charisi, A., Cheng, L. C., Jiang, T., Girke, T. ChemmineR: a compound mining framework for R. *Bioinformatics* **24**, 1733–1734 (2008).
29. Fang, Y. & Ferrie, A. M. Label-free optical biosensor for ligand-directed functional selectivity acting on β_2 adrenoceptor in living cells. *FEBS Lett.* **582**, 558–564 (2008).
30. Goral, V., Jin, Y., Sun, H., Ferrie, A. M., Wu, Q. & Fang, Y. Agonist-directed desensitization of the β_2-adrenergic receptor. *PLoS One* **6**, e19282 (2011).
31. Rutten, F. H., Zuithoff, N., Hak, E., Grobbee, D. E. & Hoes, A. W. β-blockers may reduce mortality and risk of exacerbations in patients with chronic obstructive pulmonary disease. *Arch. Intern. Med.* **170**, 880–887 (2010).
32. Penn, R. B. Agonizing over agonism: should asthmatics turn their β-receptors on or off? *Proc. Natl. Acad. Sci. USA* **106**, 2095–2096 (2009).

Author contributions

Y.F. conceived the idea, designed experiments, analyzed the data, and wrote the manuscript. A.M.F. conducted the DMR assays and analyzed the data. H.S. conducted the cAMP assays and analyzed the data.

Additional information

Supplementary Information accompanies this paper at http://www.nature.com/scientificreports

Competing financial interests: Y.F., A.M.F., and H.S. are employee and stock holders of Corning Incorporated.

How to cite this article: Ferrie, A.M., Sun, H. & Fang, Y. Label-free integrative pharmacology on-target of drugs at the β_2-adrenergic receptor. *Sci. Rep.* **1**, 33; DOI:10.1038/srep00033 (2011).